Mathematical Theory and Modeling
ISSN 2224-5804 (Paper) ISSN 2225-0522 (Online)
Vol.5, No.8, 2015

Numerical analysis of the Taylor Galerkin Pressure Correction (TGPC) finite element method for Newtonian fluid

Alaa H. Al-Muslimawi*, Sahar D. Shakir
Department of Mathematics, College of Science, University of Basra

Abstract
In this study, a time stepping Taylor Galerkin Pressure Correction finite element scheme (TGPC) is investigated on the basis of incompressible Newtonian flows. Naiver-Stoke partial differential equations have been used to describe the motion of the fluid. The equations consist of a time-dependent continuity equation for conservation of mass and time-dependent conservation of momentum equations. Examples considered include a start-up of Poiseuille flow in a rectangular channel for the Newtonian fluid. In that context, three different meshes 2×2, 5×5 and 10×10 are implemented to investigate the effect mesh refinements on the accuracy of the solution. In addition, the behaviour of velocity and pressure are reported in this study.
Keywords: Finite element methods, Taylor expansion, Naiver-Stoke equations, Newtonian fluid, Galerkin method

1. Introduction

The solution of the system of differential equations governing the flow of Newtonian fluids, has attached some considerable attention in the field of computational fluid dynamics (CFD). For a simple shear flow, under constant pressure and temperature, Newtonian fluids exhibit a linear relationship between shear stress and shear rate through a constant viscosity. The behaviour of such fluids can be predicted on the basis of the Navier-Stokes differential equations. This system is presented by the momentum (Navier-Stokes) equations. Consequently mass conservation and momentum partial differential equations are exhibited for the Newtonian case (see for example Bird et al. 1987 for details).

It is generally accepted that, throughout the history of computation, numerical simulation has advanced to address many different scientific problems. Numerical techniques have been developed to solve system of partial differential equations. However, before start solving any system of partial differential equations, we need to study and understand the physics and mathematics of such systems. Yet, the range of applications of a particular numerical technique may be problem and context dependent. For typical flow problems, it is not possible to solve such problems analytically. Throughout the history of computation, numerical investigation has advanced in addressing many different scientific problems. In this context several numerical techniques have been developed to solve systems of partial differential equations. Indeed, for such problems there are three main methods: finite difference method (FDM) (Smith 1985), finite element method (FEM) (Zinenkiewicz 1977, 1981, 1994, 2000) and finite volume method (FVM) (Versteeg & Malalasekera 2007).

Recently, the finite element method (FEM) has become the most widespread numerical scheme used to solve several scientific problems (see for example Chandrupatla & Belegundu 2002). In fact, this method is widely used in numerical procedures to solve systems of differential or integral equations (change of type of the equations and mesh refinements can improve solution accuracy). Moreover, it has been applied to a large number of physical problems. The method essentially consists of assuming a piecewise continuous form for the solution and obtaining the weights of the functions in a manner that reduces the error in the solution. In this method of analysis, a complex region defining a continuum is discretised into simple geometric shapes called finite elements. The material properties and governing

relationships are considered over these elements and expressed in terms of unknown values at element corners. An assembly process, duly considering the loading and constraints, results in a set of equations. Solution of these equations gives us the approximate behaviour of the continuum. The most suitable numerical technique within the finite element framework for solution of the differential equations is a time stepping Taylor Galerkin Pressure Correction finite element scheme (TGPC) (Townsend & Webster 1987, Hawken et al. 1990). This approach involves two distinct aspects, a Taylor–Galerkin method and a pressure-correction method. The Taylor–Galerkin method is a two-step Lax-Wendroff time stepping procedure (predictor-corrector), extracted via a Taylor series expansion in time (Donea 1984, Zinenkiewicz et al. 1985). The pressure-correction method accommodates the incompressibility constraint to ensure second-order accuracy in time (see Hawken et al. 1990, Aboubacar et al. 2002).

In this study, a time stepping Taylor Galerkin Pressure Correction finite element approach (TGPC) is employed to solve sets of differential equations. This method is described base on Taylor expansion. The scheme is applied on triangular FE meshes, with pressure nodes located at the vertices and velocity components at both vertices and mid-side nodes. Here, specific problem considered is a start-up channel flow for plane systems.

2. Mathematical modelling

Isothermal flow of an incompressible fluid can be modelled through a system of differential equations comprising those for the balance conservation of mass and momentum equations. In the absence of body forces, such a system can be written as:

$$\nabla \cdot u = 0. \tag{1}$$

Where u is the fluid velocity.

The balance of momentum reduces to

$$\rho \frac{\partial u}{\partial t} = \nabla \cdot \sigma - \rho u.\nabla u\,, \tag{2}$$

where ρ is the fluid density and σ the total-stress tensor, which equals

$$\sigma = -pI + 2\mu_s d\,. \tag{3}$$

Where p is the hydrodynamic pressure, I the unit tensor, μ_s the solvent viscosity and the Euler rate-of-deformation tensor $d = (L + L^T)/2$, with $L^T = \nabla \mathrm{u}$ the velocity gradient (for more details see Bird et al. 1987, Al-Muslimawi 2013).

The governing equations are expressed in non-dimensional terms via length scale L (unit length), velocity scale U, time scale L/U, and pressure and extra-stress scale of $\mu U/L$. Here, the dimensionless parameters are introduced in the form of Reynolds number Re, and solvent fraction β, which are given by

$$\mathrm{Re} = \rho \frac{UL}{\mu}, \quad \beta = \mu_s\,. \tag{4}$$

For Newtonian flow, the system of governing equation can be expressed in non-dimensional form as:

$$\nabla \cdot u = 0\,, \tag{5}$$

$$\mathrm{Re}\,\frac{\partial u}{\partial t} = \nabla \cdot (-pI + 2\beta d) - \mathrm{Re}\,u.\nabla u\,. \tag{6}$$

3. Numerical scheme

3.1 Time discretisation

In this study, a time stepping Taylor Galerkin Pressure Correction scheme (TGPC) has been performed. This method is developed by Townsend and Webster (Townsend & Webster 1987, Hawken et al. 1990). To describe this method, Lax_Wendroff time stepping (Strikwerda 1989) is implemented using Taylor expansion. Here, the momentum equation (6) is expressed as

$$\frac{\partial u}{\partial t} = \frac{1}{\mathrm{Re}}\left[L(u,d) - \nabla p\right], \tag{7}$$

where,

$$L(u,d) = \nabla \cdot (2\beta d) - \mathrm{Re}\, u.\nabla u\,. \tag{8}$$

A second-order Taylor expansion of u around t^n results in the following expression

$$u^{n+1} = u^n + \Delta t\left(\frac{\partial u}{\partial t}\right)^n + \frac{(\Delta t)^2}{2}\left(\frac{\partial^2 u}{\partial t^2}\right)^n,$$

thus,

$$u^{n+1} = u^n + \Delta t\left[\frac{1}{\mathrm{Re}}\left[L(u,d) - \nabla p\right]\right]^n + \frac{(\Delta t)^2}{2}\left[\frac{\partial}{\partial u}\left(\frac{1}{\mathrm{Re}}\left[L(u,d) - \nabla p\right]\right)\right]^n\left[\frac{1}{\mathrm{Re}}\left[L(u,d) - \nabla p\right]\right]^n \tag{9}$$

To obtain a $O(\Delta t^2)$ accurate method avoiding the explicit evaluation of the first derivative a two-step Lax_Wendroff scheme is applied. The first step calculates values for u(*x*, *t*) at half time steps, $t^{n+\frac{1}{2}}$ and half grid points. In the second step values at t^{n+1} are calculated using the data for t^n and $t^{n+\frac{1}{2}}$. Thus, the velocity can be written as

$$\text{Step 1: } u^{n+\frac{1}{2}} = u^n + \frac{\Delta t}{2\,\mathrm{Re}}\left[L(u^n, d^n) - \nabla p^n\right], \tag{10a}$$

$$\text{Step 2: } u^{n+1} = u^n + \frac{\Delta t}{\mathrm{Re}}\left[L(u^{n+\frac{1}{2}}, d^{n+\frac{1}{2}}) - \nabla p^{n+\frac{1}{2}}\right]. \tag{10b}$$

The pressure $p^{n+\frac{1}{2}}$ in Eq. (10b) is approximated by

$$p^{n+\frac{1}{2}} = \theta p^{n+1} + (1-\theta)p^n, \tag{11}$$

$p^{n+\frac{1}{2}}$ has an error equal to $O(\Delta t^2)$ for $\theta = 1/2$ and for other values of θ the pressure $p^{n+\frac{1}{2}}$ has an error equal to $O(\Delta t)$. The Eq. (10b) can be rewritten as

$$u^{n+1} = u^n + \frac{\Delta t}{\mathrm{Re}}\left[L(u^{n+\frac{1}{2}}, d^{n+\frac{1}{2}}) - \theta\nabla p^{n+1} - (1-\theta)\nabla p^n\right]. \tag{12}$$

In order to solve Eq. (12) together with the incompressibility constraint (5), an intermediate velocity u^* is introduced such that

$$u^* = u^n + \frac{\Delta t}{\mathrm{Re}}\left[L(u^{n+\frac{1}{2}}, d^{n+\frac{1}{2}}) - \nabla p^n\right]. \tag{13}$$

From Eq.(12) and Eq.(13), u^{n+1} is given as

$$u^{n+1} = u^* - \frac{\theta\Delta t}{\mathrm{Re}}\nabla(p^{n+1} - p^n), \tag{14}$$

Taking the divergence of Eq. (13), and using $\nabla \cdot u^{n+1} = 0$, gives the pressure difference $(p^{n+1} - p^n)$ as function of u^* only:

$$\nabla^2(p^{n+1} - p^n) = \frac{\mathrm{Re}}{\theta\Delta t}\nabla \cdot u^*, \tag{15}$$

Then, the fractional-staged formulations within each time-step may be given by

Stage 1a: $$\frac{2\,\mathrm{Re}}{\Delta t}(u^{n+\frac{1}{2}} - u^n) = \left[L(u^n, d^n) - \nabla p^n\right], \tag{16a}$$

Stage 1b: $$\frac{\mathrm{Re}}{\Delta t}(u^* - u^n) = \left[L(u^{n+\frac{1}{2}}, d^{n+\frac{1}{2}}) - \nabla p^n \right], \tag{16b}$$

Stage 2: $$\nabla^2(p^{n+1} - p^n) = \frac{\mathrm{Re}}{\theta\Delta t}\nabla \cdot u^*, \tag{16c}$$

Stage 3: $$u^{n+1} = u^* - \frac{\theta\Delta t}{\mathrm{Re}}\nabla(p^{n+1} - p^n). \tag{16d}$$

3.2 Finite element scheme

In the finite element method, we introduce approximations $u(x,t)$ and $p(x,t)$ to the velocity and pressure respectively over finite dimensional function spaces. Hence we have,

$$u(x,t) = u_j(t)\phi_j(x), \quad j = 1,\cdots.6, \qquad p(x,t) = p_k(t)\psi_k(x), \quad k = 1,\cdots,3. \tag{17}$$

such that $u_j(t)$ and $p_k(t)$ represent the vector of nodal values of velocity and pressure and $\phi_j(x)$, $\psi_k(x)$ are their respective basis (shape or interpolation) functions. Similar forms apply for u^* and pressure difference. The domain Ω is partitioned into triangular elements with velocities computed at the vertex and midside nodes, and pressure only at vertex nodes. For the shape functions, $\phi_j(x)$ are selected as piecewise quadratic basis functions and $\psi_k(x)$ as piecewise linear basis functions. The corresponding semi-implicit Taylor-Galerkin/Pressure-Correction (TGPC) form of equations ((16a), (16b), (16c) and (16d)) may then be expressed in matrix-form as (see Baloch et al. 1995, Al-Muslimawi et al. 2013):

Step 1a: $$[\frac{2\,\mathrm{Re}}{\Delta t}M + \frac{1}{2}S](U^{n+\frac{1}{2}} - U^n) = \{-[S + \mathrm{Re}\,N(U)]U + L^T P\}^n, \tag{18a}$$

Step 1b: $$[\frac{\mathrm{Re}}{\Delta t}M + \frac{1}{2}S](U^* - U^n) = \{-SU + L^T p\}^n - \mathrm{Re}[N(U)U]^{n+\frac{1}{2}}, \tag{18b}$$

Step 2: $$K(P^{n+1} - P^n) = -\frac{\mathrm{Re}}{\theta\,\Delta t}LU^*, \tag{18c}$$

Step 3: $$\frac{\mathrm{Re}}{\Delta t}M(U^{n+1} - U^*) = \theta L^T(P^{n+1} - P^n). \tag{18d}$$

Where, M is the mass matrix, S is the momentum diffusion matrix, K is the pressure stiffness matrix, $N(U)$ is the convection matrix and L is the divergence/ pressure gradient matrix. In the matrix notation

$$M_{ij} = \int_{\Omega} \phi_i . \phi_j \, d\Omega \quad , \; K_{ij} = \int_{\Omega} \nabla \psi_i \nabla \psi_j \, d\Omega \quad , \quad N(U)_{ij} = \int_{\Omega} \phi_i \, (U_k^l \frac{\partial \phi_j}{\partial x_k}) \, d\Omega$$

$$(L)_{ij} = \int_{\Omega} \psi_i \frac{\partial \phi_j}{\partial x_k} \, d\Omega \quad , (S)_{ij} = \int_{\Omega} \frac{\partial \phi_i}{\partial x_k} \frac{\partial \phi_j}{\partial x_k} + (\frac{\partial \phi_j}{\partial x_k})^T \, d\Omega$$

4. Problem specification

In this study, Poiseuille flow along a 2d planar straight channel, under isothermal condition is studied. Here, the comparative study of analytic solution of Naiver-Stokes equations under special cases with the numerical results is conducted. Additionally, in the present study a finite small value of the Reynolds number is assumed, Re= 10^{-4} and the time-stepping procedure is monitored for convergence to a steady state via relative norms subject to satisfaction of a suitable tolerance criteria taken here as 10^{-10} with typical Δt is $O(10^{-3})$.

4.1 Exact solutions of Naiver-Stokes equations for parallel flow

Finding exact solution of Naiver-Stokes equations, displays mathematical difficulties because of the nonlinear terms of equations (Cuvelier et al. 1986). However, it is possible to find analytical solutions in certain particular cases, generally when the nonlinear convective terms vanish naturally. Parallel flows, in which only one velocity component is different from zero, of a two dimensional, incompressible fluid have this characteristic. In order to illustrate this concept, consider two dimensional steady incompressible flows in channel with straight parallel sides (see Figure 1).

Under these assumptions, the continuity and momentum equations in the absence of body force can be expressed as:

Continuity

$$\frac{\partial u}{\partial x} + \frac{\partial v}{\partial y} = 0 . \tag{19}$$

Momentum

$$\rho(u\frac{\partial u}{\partial x} + v\frac{\partial u}{\partial y}) = -\frac{\partial P}{\partial x} + \mu(\frac{\partial^2 u}{\partial x^2} + \frac{\partial^2 u}{\partial y^2}) \qquad \text{(x-direction)} \tag{20}$$

$$\rho(u\frac{\partial v}{\partial x} + v\frac{\partial v}{\partial y}) = -\frac{\partial P}{\partial y} + \mu(\frac{\partial^2 v}{\partial x^2} + \frac{\partial^2 v}{\partial y^2}) \qquad \text{(y-direction)} \tag{21}$$

Since the flow is constrained by the flat parallel walls of the channel, no components of velocity in y-direction is possible (v=0). Consequently, $\frac{\partial v}{\partial x} = \frac{\partial v}{\partial y} = \frac{\partial^2 v}{\partial^2 x} = \frac{\partial^2 v}{\partial^2 y} = 0 .$

Thus, from continuity equation we obtain,

$$\frac{\partial u}{\partial x} = -\frac{\partial v}{\partial y} = 0 , \tag{22}$$

which leads to get,

$$\frac{\partial u}{\partial x} = \frac{\partial^2 u}{\partial^2 x} = 0. \tag{23}$$

Also, the momentum equation can be reduced to

$$\frac{\partial P}{\partial x} = \mu \frac{\partial^2 u}{\partial y^2}, \tag{24}$$

$$\frac{\partial P}{\partial x} = 0. \tag{25}$$

The differential equation (24) can be solved by integration with respect to y to get

$$u(y) = \frac{1}{2\mu}\frac{\partial P}{\partial x} y^2 + C_1 y + C_2. \tag{26}$$

By applying no-slip boundary conditions at the walls, we have

$$\begin{aligned} y = h \quad &\Rightarrow \quad u = 0 \\ y = 0 \quad &\Rightarrow \quad u = 0 \end{aligned} \tag{27}$$

By using these boundary conditions, the integration constants C_1 and C_2 can be evaluated to have

$$C_1 = -\frac{h}{2\mu}\frac{\partial P}{\partial x}, \quad C_2 = 0. \tag{28}$$

Therefore, the general solution of equation (24) is enforced as

$$u(y) = \frac{1}{2\mu}\frac{\partial P}{\partial x} y^2 - \frac{h}{2\mu}\frac{\partial P}{\partial x} y = -\frac{h}{2\mu}\frac{\partial P}{\partial x} y(1 - \frac{y}{h}). \tag{29}$$

The maximum velocity, which occurs at the centre of the channel (at $y = \frac{h}{2}$), is expressed as

$$u_{\max} = -\frac{h^2}{8\mu}\frac{\partial P}{\partial x}. \tag{30}$$

Introducing the non-dimensional variables, $\bar{u} = \frac{u}{u_{\max}}$ and $\bar{y} = \frac{y}{h}$ gives the general solution of equation (24) in the non-dimensional form

$$\bar{u} = 4\bar{y}(1 - \bar{y}). \tag{31}$$

4.2 Numerical discretisation

A time fractional-staged Taylor-Galerkin incremental pressure-correction (TGPC) framework is considered. In that context, a structured, uniform, quadrilateral-based, triangular finite element mesh has been used, for the 2×2 mesh as displayed in Figure 2a. To test for accuracy, a similar meshes consisting of 5×5 and 10×10 have been used (see Figure 2(b,c)). Typical finite element mesh characteristics are included in Table 1.

Boundary conditions: The boundary conditions for the study are illustrated in Figure 3. Poiseuille flow is specified at the inlet, and no-slip boundary condition is imposed on the channel wall. Along the outflow boundary, zero radial velocity applies.

5. Numerical results

5.1 Rate of convergence

History plots of the relative error increment norms in velocity and pressure are provided in Figure 4 for the three different structure meshes 2×2, 5×5 and 10×10. These results reflect a superior rate of convergence for all solution components under the 10×10 mesh compared to

2×2 and 5×5 meshes. As a consequence, large time-steps are required under the 10×10 mesh to reach an equitable level of tolerance, as opposed to with the alternative meshes. Note, the same rate of convergence in velocity and pressure components is shown with all meshes. In summary, one can conclude that the 10×10 mesh provides better convergence in contrast to others meshes due to the number of elements.

5.2 Velocity fields and profiles

Figure 5 demonstrates axial velocity fields v_x and vector for Newtonian flow based on three difference meshes 2×2, 5×5 and 10×10. Comparative graphical data on velocity changes for these meshes are shown in Figure 5. The results reveal that, the maximum in v_x field plot is located at the middle of the channel, while minimum level of the velocity occurred near the walls. Here, one can see clearly the effect of the element number of the mesh on the accuracy of the results, where 5×5 and 10×10 meshes comparatively more accurate than the 2×2 mesh (see Table 2). The corresponding profile with zoomed representation for axial velocity in fully developed flow is provided in Figure 6. The comparison in velocity between the numerical solution and exact solution for 2d planar straight channel is displayed for three structured meshes. For all cases, the cross-channel axial velocity profile shows parabolic flow structure. Findings reveal that, the results for 5×5 and 10×10 meshes are closed to the exact solution compared to 2×2 mesh due to the increasing in the number of mesh elements.

5.3 Pressure fields

In Figure 7 fields plot are presented for pressure P for 2×2 and 10×10 meshes. As to be anticipated, a distinct level of pressure rise along the inlet of channel decreasing whenever closer from the outlet of the channel. From these fields, one can observe the maximum levels of P for 2×2, 5×5 and 10×10 meshes are 12 units, 16 units and 16.0002 units, respectively, (see Table 2). In addition, more accuracy in the pressure results is appeared for 10×10 mesh compared to 2×2 mesh due to mesh refinement.

6. conclusion

In this study, we have employed a time stepping Taylor Galerkin Pressure Correction scheme (TGPC) to investigate a 2d planar straight channel (Parallel flows), under isothermal condition is studied. Accuracy and performance of the incompressible Newtonian algorithm based on mesh refinement are considered. To investigate numerical stability and accuracy properties through time-stepping (TGPC), a comparison against analytical solution is achieved under certain particular cases using three different structure meshes. We note the accuracy for the solution and time-steps increase with increasing mesh refinement.
In contrast, high level of pressure is located in the inlet of the channel, while large value of velocity is observed in the middle of channel.

References

Aboubacar, M., Matallah, H., Webster, M.F. (2002), 'Highly elastic solutions for Oldroyd-B and Phan-Thien/Tanner fluids with a finite volume/ element method: planar contraction flows' J. Non-Newtonian Fluid Mech. **103**, 65–103.

Al-Muslimawi, A., (2013), 'Numerical analysis of partial differential equations for viscoelastic and free surface flows, PhD thesis, University of Swansea

Al-Muslimawi, A., Tamaddon-Jahromi, H.R., Webster, M.F. (2013), 'Numerical simulation of tube tooling cable-coating with polymer melts', The 13th International Symposium on Applied Rheology (ISAR), The Korean Society of Rheology, 31 – 55.

Baloch, A., Townsend, P., Webster, M.F. (1995),'On two and three dimensional expansion flows', Computers and Fluids, **24**(8), 863-882.

Bird, R. B., Armstrong, R.C., Hassager, O., (1987),'Dynamic of polymeric liquids', Volume 1: Fluid mechanic, nJohn Wiles & Sons, Inc.

Chandrupatla, T.R., Belegundu, A.D. (2002),'Introduction to finite elements in engineering', Pearson Prentice Hall.

Cuvelier, C., Segal, A., Van Steenhoven, A.A. (1986),'Finite Difference method and Naiver-Stokes Equations', D. Reidel Publishing Company.

Donea, J. (1984),'A Taylor–Galerkin method for convective transport problems, Int. J. Num. Meth. Eng. **20**, 101–119.

Hawken, D.M., Tamaddon-Jahromi, H.R., Townsend, P., Webster, M.F.(1990),'A Taylor Galerkin-based algorithm for viscous incompressible flow', Int. J. Num. Meth. Fluids **10**, 327-351.

Smith, G.D.(1985).'Numerical solution of partial differential equations: Finite difference methods', Oxford University Press.

Strikwerda, J.C.(1989),' Finite Difference Scheme and Partial Differential Equations', Chapman & Hall, New York, NY.

Townsend, P., Webster, M.F.(1987).'An algorithm for the three-dimensional transient simulation of non-Newtonian fluid flows', in: M.J.G.N. Pande, G.N. Nijhoff (Eds.), Transient/Dynamic Analysis and Constitutive Laws for Engineering Materials International Conference on Numerical Methods in Engineering: Theory and Applications NUMETA 87, vol. 2, T12/1-11, Kluwer, Dordrecht, pp. 1–11.

Versteeg, H.K., Malalasekera, W.(2007).'An introduction to computational fluid dynamics: The finite volume method', Pearson Prentice Hall.

Zinenkiewicz, O. C.(1977),'The finite element method', McGraw-Hill, London.

Zinenkiewicz, O. C.(1981),' The finite element method', McGraw-Hill.

Zinenkiewicz, O. C., Taylor. (1994),'The finite element method', vol. 1: McGraw-Hill.

Zinenkiewicz, O. C., Taylor. (2000),'The finite element method', vol1: The basis, Butterworth-Heinemann, 5th edition.

Zinenkiewicz, O. C., Morgan, K., Peraire, J., Vandati, M., Löhner, R.(1985).'Finite elements for compressible gas flow and similar systems', in: Proceedings of the 7th International Conference on Comput. Meth. Appl. Sci. Eng., Versailles, France.

List of Tables

List of Figures

Figure 4: History of the relative error increment norms in velocity and pressure

Figure 5: Axial velocity fields: (a) 2×2 mesh, (b) 5×5 mesh, (c) 10×10 mesh

Figure 6: Cross-channel axial velocity profiles: 2×2 mesh, 5×5 mesh, 10×10 mesh and analytic solution

Figure 7: Pressure fields: (a) 2×2 mesh, (b) 10×10 mesh

Table 1: Mesh characteristic parameters

Mesh	Total Element	Total Nodes	Boundary Nodes	Pressure Nodes
2×2	8	25	16	9
5×5	50	121	40	36
10×10	200	441	80	121

Table 2: Axial velocity, pressure

Mesh	V_x	P
2×2	Max=1 Min=0	Max=12.6999 Min=0
5×5	Max=1 Min=0	Max=16 Min=0
10×10	Max=1 Min=0	Max=16.0002 Min=0

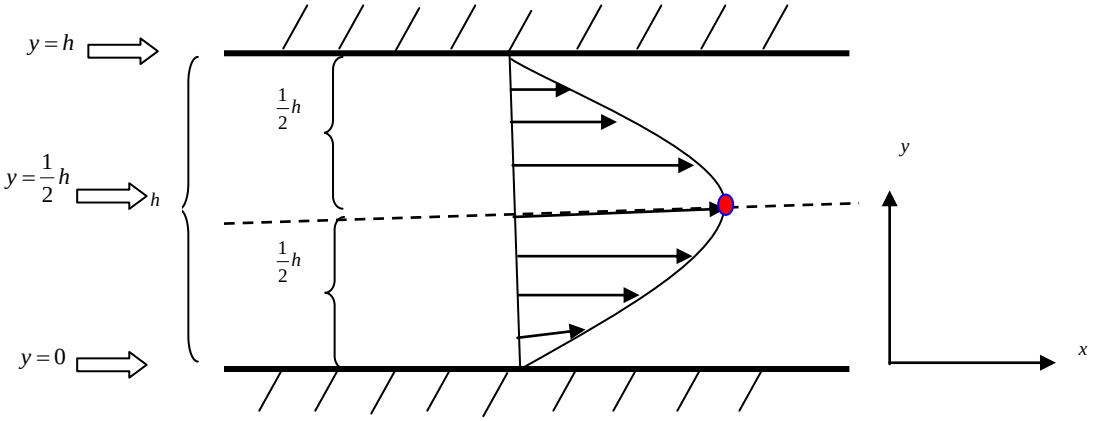

Figure 1: Parallel flows in channel

(a)

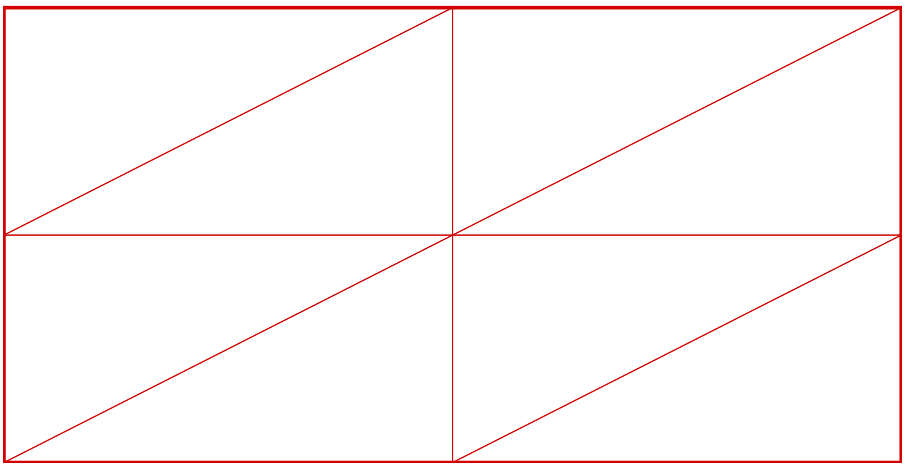

(b)

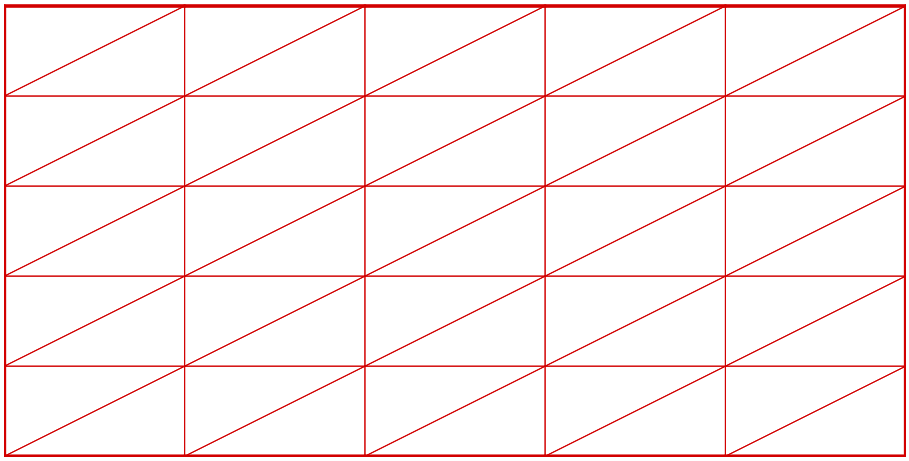

(c)

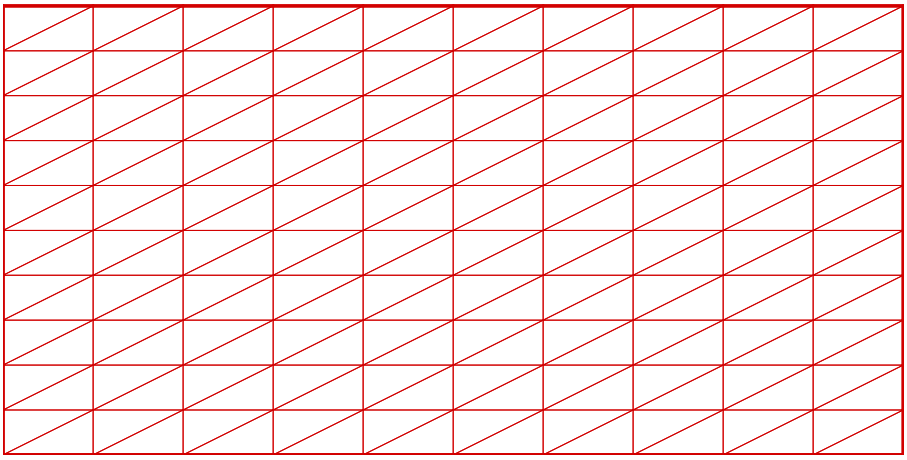

Figure 2: (a) Structured 2×2 finite element mesh, (b) Structured 5×5 finite element mesh, (c) Structured 10×10 finite element mesh

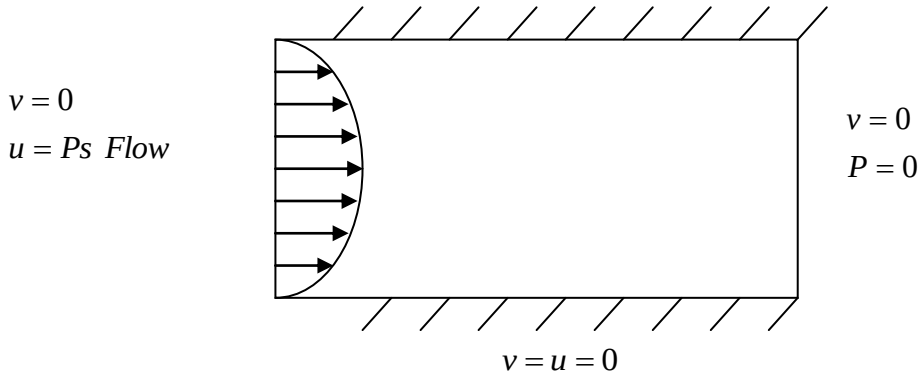

Figure 3: Schema for flow problem, boundary conditions

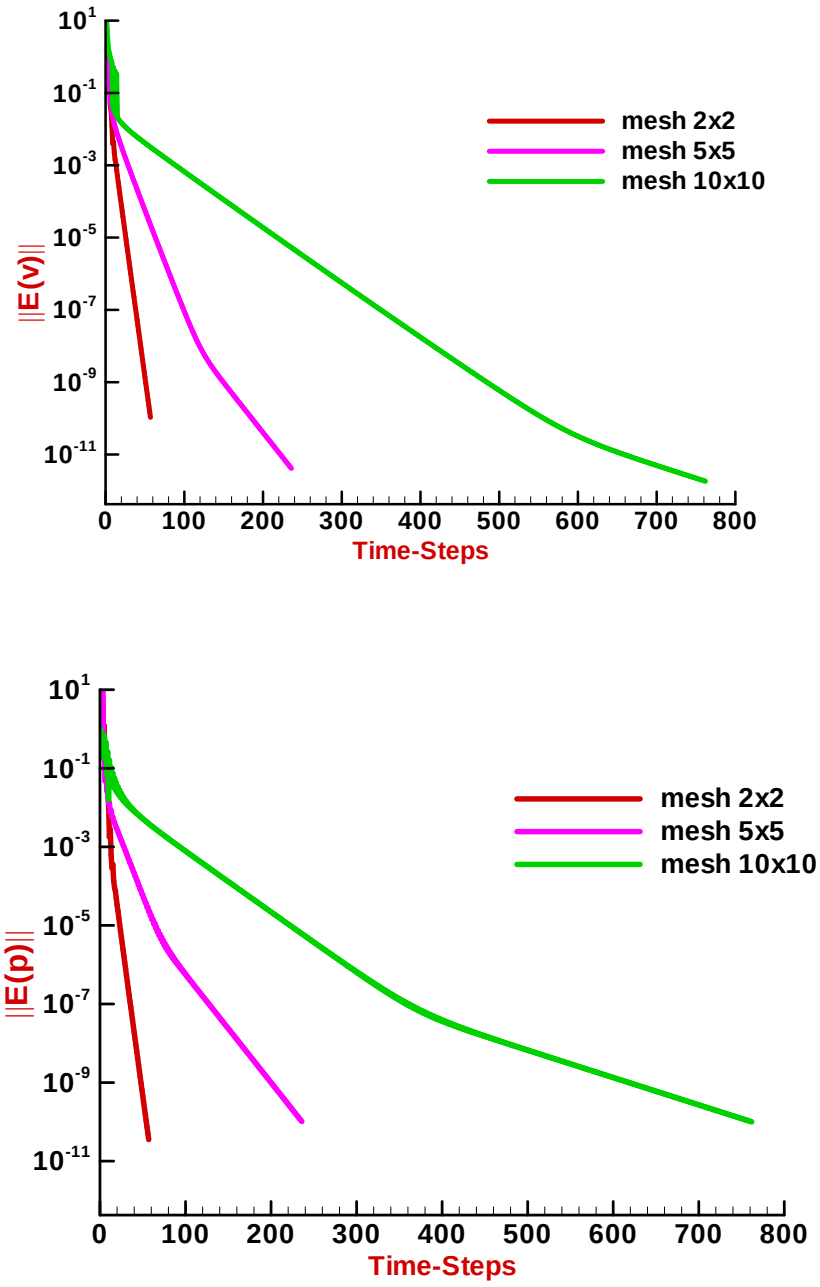

Figure 4: History of the relative error increment norms in velocity and pressure

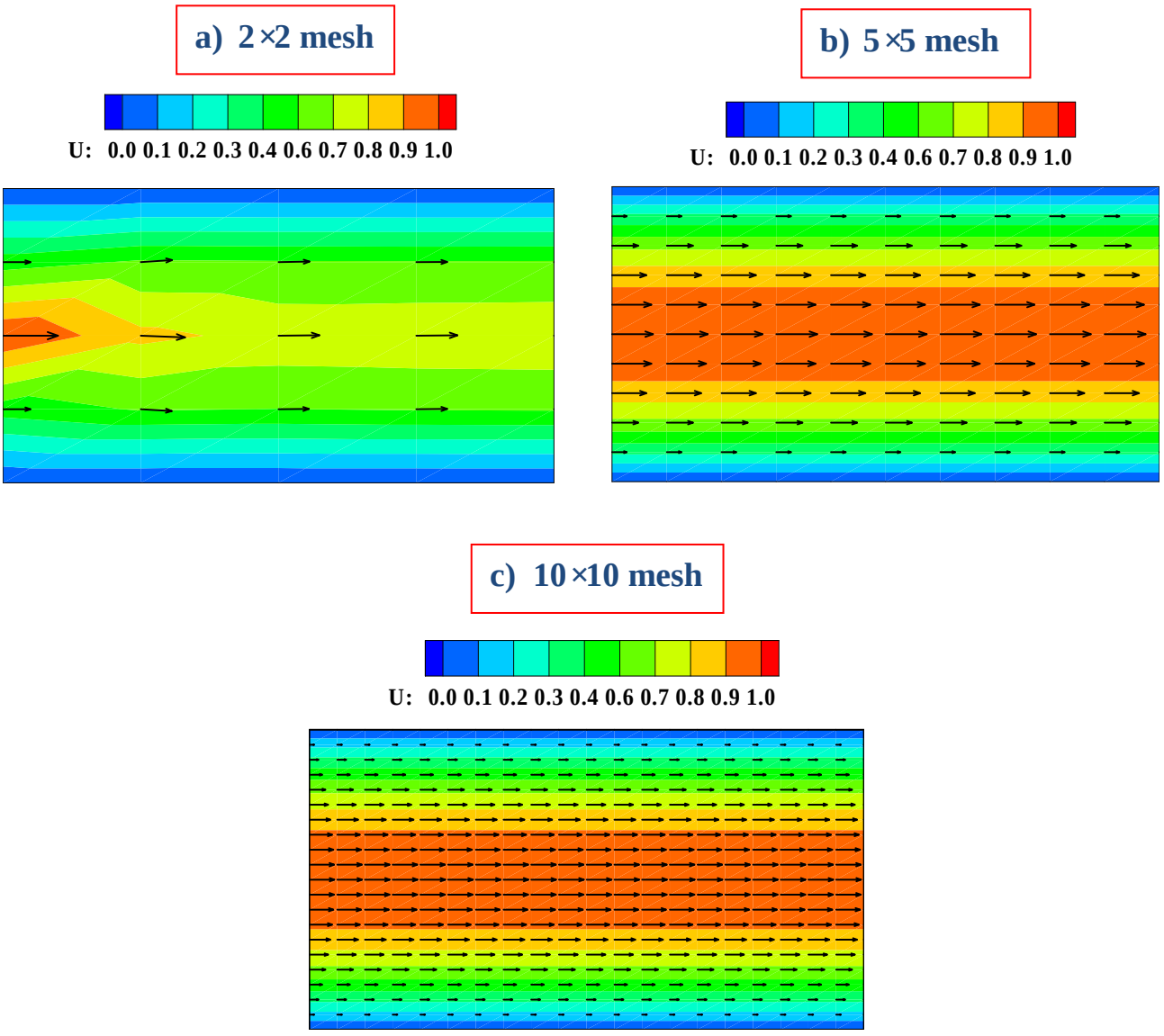

Figure 5: Axial velocity fields: (a) 2×2 mesh, (b) 5×5 mesh, (c) 10×10 mesh

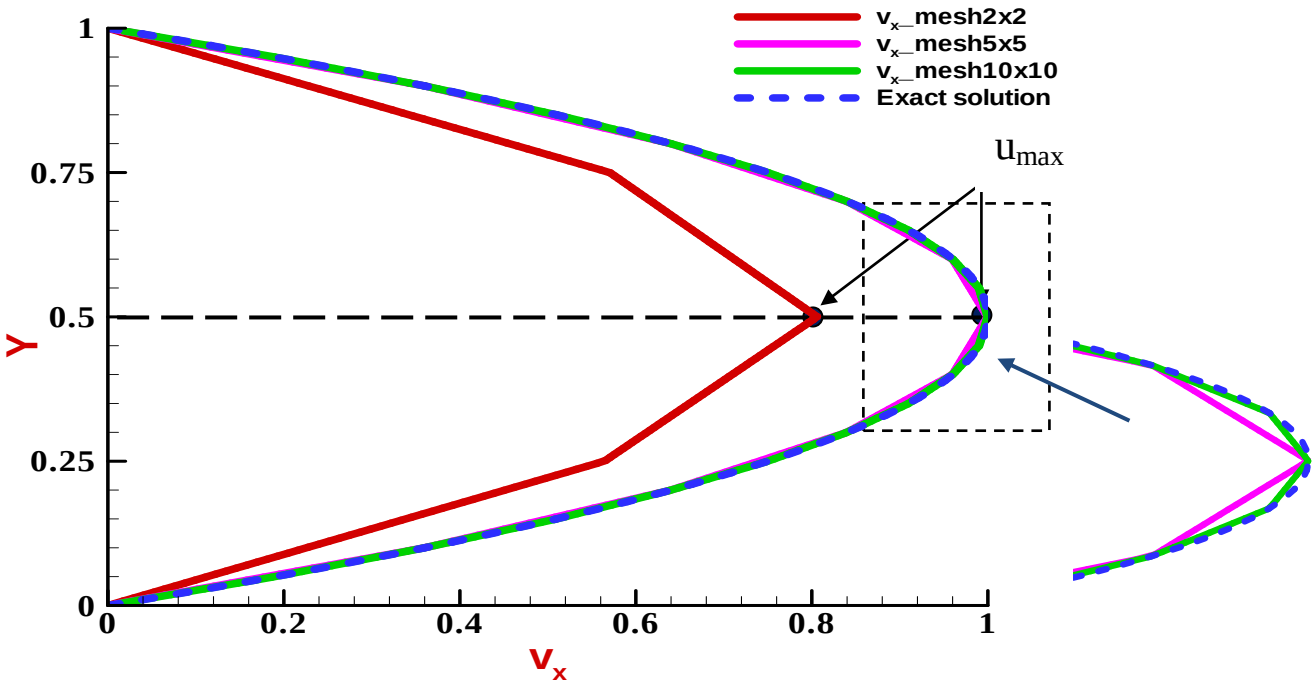

Figure 6: Cross-channel axial velocity profiles: 2×2 mesh, 5×5 mesh, 10×10 mesh and analytic solution

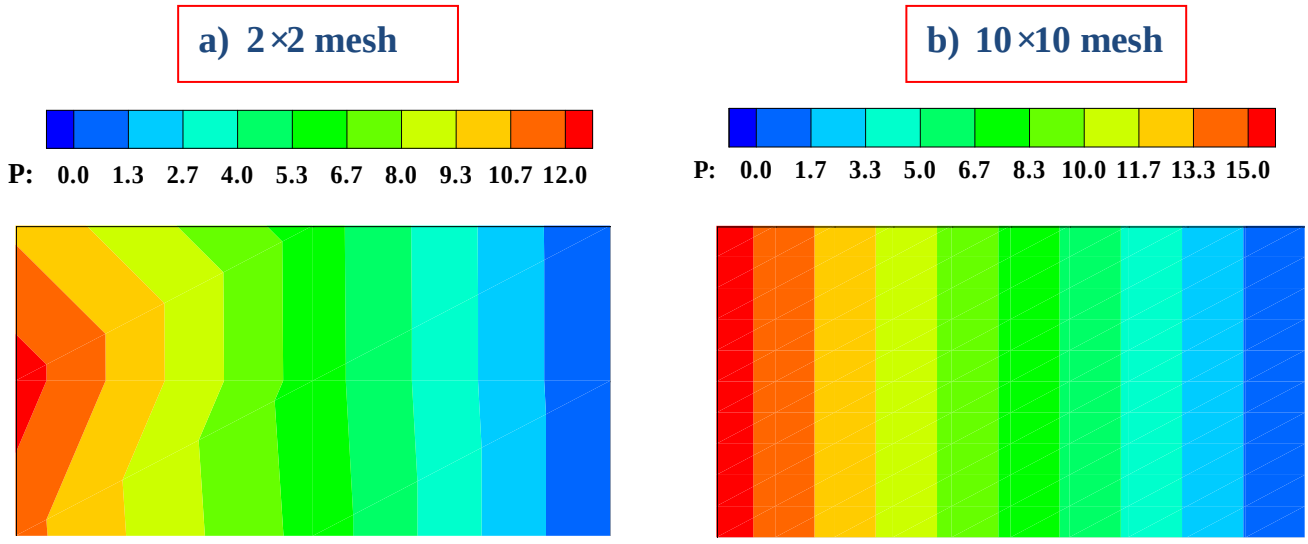

Figure 7: Pressure fields: (a) 2×2 mesh, (b) 10×10 mesh

The IISTE is a pioneer in the Open-Access hosting service and academic event management. The aim of the firm is Accelerating Global Knowledge Sharing.

More information about the firm can be found on the homepage:
http://www.iiste.org

CALL FOR JOURNAL PAPERS

There are more than 30 peer-reviewed academic journals hosted under the hosting platform.

Prospective authors of journals can find the submission instruction on the following page: http://www.iiste.org/journals/ All the journals articles are available online to the readers all over the world without financial, legal, or technical barriers other than those inseparable from gaining access to the internet itself. Paper version of the journals is also available upon request of readers and authors.

MORE RESOURCES

Book publication information: http://www.iiste.org/book/

Academic conference: http://www.iiste.org/conference/upcoming-conferences-call-for-paper/

IISTE Knowledge Sharing Partners

EBSCO, Index Copernicus, Ulrich's Periodicals Directory, JournalTOCS, PKP Open Archives Harvester, Bielefeld Academic Search Engine, Elektronische Zeitschriftenbibliothek EZB, Open J-Gate, OCLC WorldCat, Universe Digtial Library , NewJour, Google Scholar